

Cesium satellite band at 875.2 nm stemming from the $\text{Cs}_2 0_g^+(6p\ ^2P_{1/2} + 6s\ ^2S_{1/2})$ state

 R. Beuc^{1,a}, H. Skenderović¹, T. Ban¹, D. Veža¹, G. Pichler¹, and W. Meyer²
¹ Institute of Physics, P.O. Box 304, 10000 Zagreb, Croatia

² Fachbereich Chemie, Postfach 3049, 67653 Kaiserslautern, Germany

Received 07 March 2001 and Received in final form 14 May 2001

Abstract. We measured a very distinct satellite band at 875.2 nm between two resonance lines of cesium. Spectral simulation using Spies and Meyer [1] *ab initio* potential curves and an appropriate transition dipole moment function was compared with experimental profile. Implications of the investigated satellite band at 875.2 nm in the field of ultracold cesium atom collisions are discussed with a special emphasize to new possibilities of the photoassociation of two ground state atoms leading to the formation of ultracold intermediate long-range molecules.

PACS. 33.70.Jg Line and band widths, shapes, and shifts – 34.20.Cf Interatomic potentials and forces

1 Introduction

The self-broadening of the first cesium resonance lines was widely investigated experimentally and theoretically [2–5]. The results of resonance broadening experiments are mostly used for testing the different theoretical models, for the determination of the accuracy of the calculated *ab initio* potential curves and for the diagnostics of high-pressure lamps.

Interaction energies, *i.e.* potential energy curves of two Cs atoms can be classified as in potassium case [6] as: short range ($5 \text{ Bohr} \leq R \leq 16 \text{ Bohr}$), intermediate range [7] ($16 \text{ Bohr} \leq R \leq 30 \text{ Bohr}$) and long-range ($R \geq 30 \text{ Bohr}$). During the past decade the accurate determinations of the molecular intermediate and long-range potentials played crucial role in the interpretation of many new physical phenomena associated with the cold atom collisions and ultracold molecules. In this paper we are dealing with the Cs_2 intermediate molecular states stemming from $6\ ^2S_{1/2} + 6\ ^2P_{1/2}$ and $6\ ^2S_{1/2} + 6\ ^2P_{3/2}$ asymptotes.

The first discussion on the origin of these satellite bands in the far quasistatic wings of the Cs resonance line was reported in reference [8]. Quite recently Veža *et al.* [9] reported on the blue satellite bands of cesium 852.1 nm line at 817 nm, 827 nm and 835 nm as stemming from the maxima in difference potential curves of the $1(a)\ ^3\Sigma_u^+(1_u, 0_u^-) \rightarrow 1\ ^3\Pi_g(2_g, 1_g, 0_g^+, 0_g^-)$ electronic transitions (Fig. 1a). Here, we are using Hund's case (a) and (c) (in brackets) designations [10]. Upper electronic

$2_g, 1_g, 0_g^+$ and 0_g^- states have the same $6\ ^2S_{1/2} + 6\ ^2P_{3/2}$ asymptote. The authors devoted a special discussion to the $1_u \rightarrow 0_g^+$ transition, since the corresponding difference potential curve has two maxima and one minimum at about 17 Bohr, which produces interesting features in the observed absorption spectrum (cusp satellite bands).

In Figure 1a Cs_2 potential curves [1] needed for the interpretation of the 875.2 nm band are shown. $\text{Cs}_2\ 1\ ^3\Pi_g$ and $2\ ^1\Sigma_g^+$ potential curves calculated without the inclusion of the spin-orbit interaction and classified as the Hund's case (a), are represented by dashed lines. Full lines represent 0_g^+ adiabatic potential curves calculated with inclusion of spin-orbit interaction and classified according to the notation of the Hund's case (c). The spin-orbit interaction removes the degeneracy at the crossing point and because of the well-known Neumann-Wigner theorem [11] an avoided crossing appears between the two 0_g^+ potential curves at the internuclear distance around 21 Bohr. This avoided crossing produces extrema in the potential curves of both 0_g^+ states. The maximum in the 0_g^+ potential curve stemming from the $6s\ ^2S_{1/2} + 6p\ ^2P_{1/2}$ asymptote is responsible for the formation of the 875.2 nm satellite band, treated in this paper experimentally and theoretically. In what follows this state will be denoted by $0_g^+(6s\ ^2S_{1/2} + 6p\ ^2P_{1/2})$.

It is interesting to note that the maximum in $0_g^+(6\ ^2S_{1/2} + 6\ ^2P_{1/2})$ potential curve is essentially a potential barrier that splits bound states at shorter distances and continuum states at larger distances of the interacting cesium atoms (see Fig. 1a). In order to obtain relevant molecular electronic dipole transition moments and

^a e-mail: beuc@ifs.hr

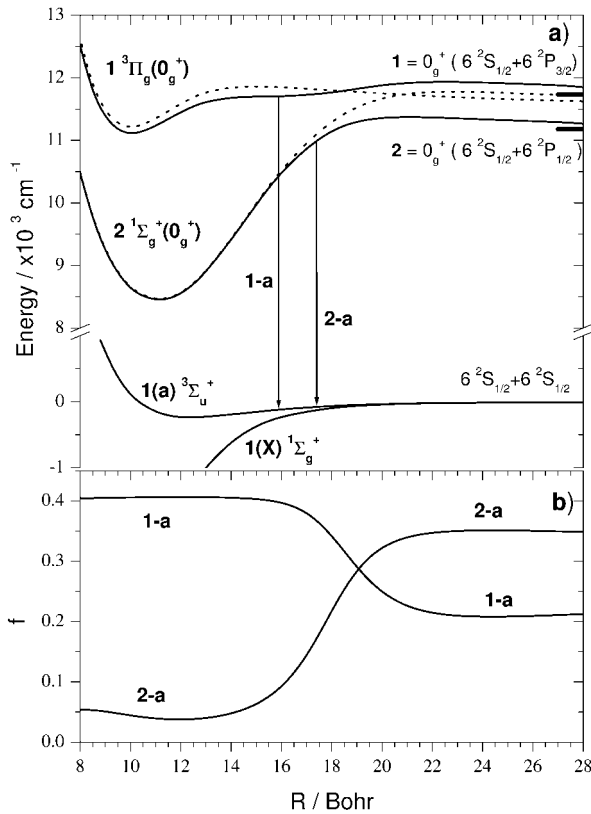


Fig. 1. (a) Cs_2 potential curves needed for the interpretation of the 875.2 nm satellite band: (full lines) with the inclusion of spin-orbit interaction, (dashed lines) without inclusion of spin-orbit interaction [1]. 1 and 2 represent adiabatic potential 0_g^+ ($6^2S_{1/2} + 6^2P_{1,2,3/2}$), having asymptotes ($6^2S_{1/2} + 6^2P_{3/2}$) and 0_g^+ ($6^2S_{1/2} + 6^2P_{1/2}$), respectively. (b) The molecular oscillator strengths f plotted as a function of the internuclear distance R for the 1-a and 2-a transitions (shown by arrows in (a)). For the sake of simplicity the lowest triplet potential $a^3\Sigma_u^+$ is denoted with a .

corresponding molecular oscillator strengths, a semi-empirical “atoms in molecules” scheme developed by Cohen and Schneider [12] was used. In Figure 1b the molecular oscillator strengths f as a function of the internuclear distance R for both 0_g^+ states are shown. At larger distances the electronic transition between 0_g^+ ($6^2S_{1/2} + 6^2P_{1/2}$) state and $1(a)^3\Sigma_u^+(1_u)$ state is allowed. At shorter distances the Cs_2 0_g^+ ($6^2S_{1/2} + 6^2P_{1/2}$) state has $1\Sigma_g^+$ symmetry, and because of selection rules the transition into the ground Cs_2 $1(X)^1\Sigma_g^+$ and the excited $1(a)^3\Sigma_u^+$ states is forbidden. Therefore at the short range, the 0_g^+ ($6^2S_{1/2} + 6^2P_{1/2}$) state is a “dark” state, except close to the barrier at about 21 Bohr. Thus, any excitation into this state close to the barrier provides a reservoir of excited, energetic molecules. The latter can serve as an intermediate “metastable” state. Two color excitation to higher excited states is an important process in the ultra cold collisions of cesium atoms.

2 Experiment

We performed absorption measurements with the cesium all-sapphire cell (ASC) [13] and the emission measurements with the high pressure Cs lamp (OSRAM, Germany).

The ASC is cylindrical in shape with an internal diameter of 10 mm, wall thickness of 3 mm and length of 160 mm. Inside the ASC is a tablet of powders that provides 0.6 mg of pure cesium. The temperature was measured by a thermocouple positioned at the middle point of the ASC. The detailed description of the cesium ASC and the experimental setup for the absorption measurements was given in previous papers [14–16]. The continuous light from a halogen lamp irradiated the ASC. The light passing through the absorption cell was spectrally analyzed using a Jobin Yvon THR 1.5 m grating spectrometer equipped with a holographic grating (1200 grooves/mm) and detected with the Hamamatsu S1336-44BQ silicon photodiode. The photodiode output signal was fed into a lock-in amplifier (Stanford Research SR510) and stored in a personal computer.

High-pressure cesium vapor lamp (OSRAM) used for the emission measurements was operated at the power of 80 W and 50 Hz AC. The burner of the lamp is a cylindrical tube made of the translucent alumina and filled with Cs and Xe [17]. In order to obtain time-resolved spectra from the sinusoidally driven plasma, the Boxcar Averager (Model 162 and 164, Princeton Applied Research) was used for processing the signal from the photodiode. The emission spectra at the current maximum point and at the current reversal point were taken.

2.1 Emission spectra

Emission spectra from the lamp are rather complex because of the thermal nonuniformity of the plasma column inside the burner. The central part of the plasma column is hotter than the outer part, so the emitted light from the core is partially absorbed in the outer layers of the column. At the current maximum point the plasma temperature and the electron density attain the largest values and therefore excited levels in Cs atoms are substantially populated even in outer layers of the burner. At the current reversal point, cesium plasma becomes much colder (the electron temperature is at minimum value).

The emission spectrum from the lamp taken at the current maximum is shown in Figure 2a. Atomic lines belonging to the sharp and diffuse series are easily identified on the elevated thermal background mainly consisting of the very far resonance line wings emission. There is huge absorption at positions of D1 and D2 resonance lines (894.3 and 852.1 nm). Due to the large population of the first excited state in cesium atom, $6^2P_{1/2,3/2}$, some of the lines ending at resonance levels are self-reversed. Atomic lines coming from $4^2F_{5/2} \rightarrow 5^2D_{3/2}$ (1002.4 nm), $4^2F_{5/2} \rightarrow 5^2D_{5/2}$, and $4^2F_{7/2} \rightarrow 5^2D_{5/2}$ (1012.3 nm) transitions are also self-reversed. The 875.2 nm satellite overlaps with the atomic line at 876.1 nm that comes

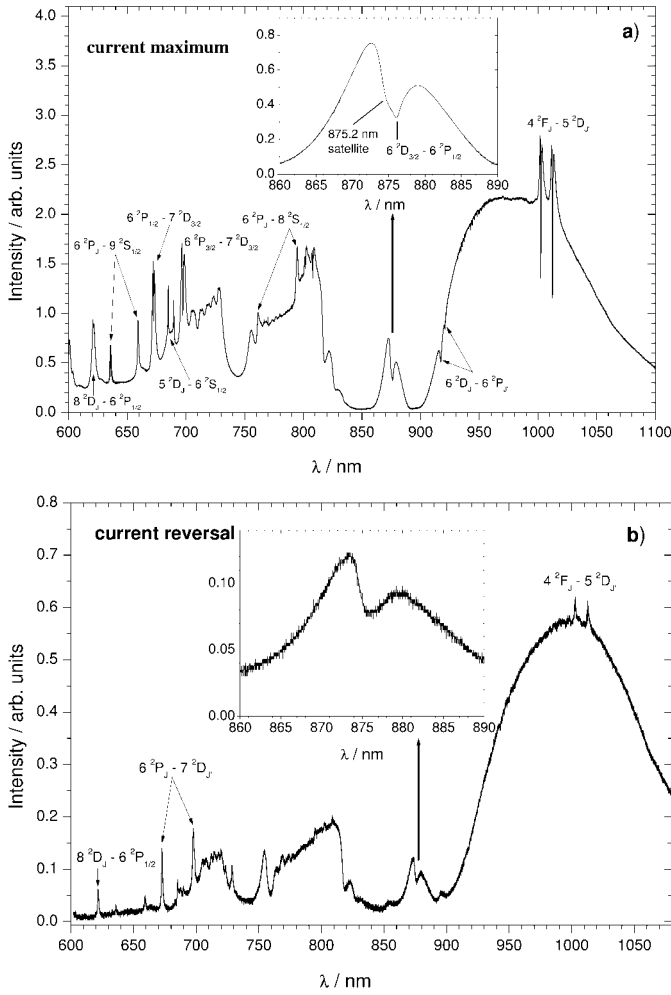


Fig. 2. The emission spectrum from the Cs high-pressure lamp: (a) current maximum and (b) current reversal. Atomic lines belonging to sharp ($n\ ^2S_{1/2} \rightarrow 6\ ^2P_J$, $n = 8, 9$) and diffuse ($n\ ^2D_{J'} \rightarrow 6\ ^2P_J$, $n = 6, 7, 8$) series together with $4\ ^2F_{J'} \rightarrow 5\ ^2P_J$ and $5\ ^2D_{J'} \rightarrow 6\ ^2S_{1/2}$ transitions are easily identified in both spectra. Satellite bands of the Cs D2 ($6\ ^2S_{1/2} + 6\ ^2P_{3/2}$) line at 817 nm, 827 nm and 835 nm and Cs_2 875.2 nm satellite band are clearly visible.

from the $6\ ^2D_{3/2} \rightarrow 6\ ^2P_{1/2}$ transition (inset in Fig. 2a). The absorption profiles of blue satellite bands [9] of the 852.1 nm line at 817 nm, 827 nm and 835 nm are also clearly pronounced in Figure 2a.

In the spectrum measured at the current reversal point, the atomic line at 876.1 nm is absent and the 875.2 nm satellite is more clearly observed (Fig. 2b and inset). The overall emission from the lamp is much weaker. The shape of the self-absorbed 875.2 nm satellite band measured by a high pressure lamp at a current reversal point and its shape in the absorption spectrum measured with ASC are similar, but the former one is much more pronounced due to larger atom density in the burner of the high pressure lamp. For further analysis of the satellite band and its comparison with the theoretical simulation, the absorption measurements with ASC were used

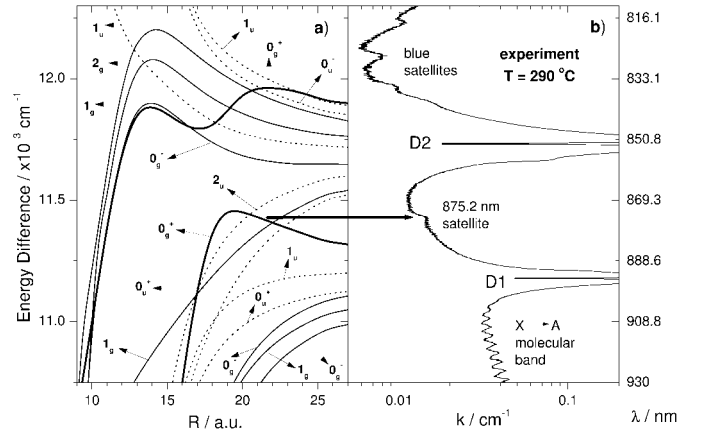


Fig. 3. (a) Cs + Cs difference potentials stemming from the $6\ ^2S_{1/2} + 6\ ^2P_{1/2}$ and $6\ ^2S_{1/2} + 6\ ^2P_{3/2}$ atomic asymptotes at intermediate internuclear distances. Each difference potential is labeled by the upper potential, while the lower potential curve is the $\text{Cs}_2 X\ ^1\Sigma_g^+(0_g^+)$ state for upper ungerade states (dashed lines), and the lower potential curve is the $\text{Cs}_2 a\ ^3\Sigma_u^+(0_u^-, 1_u)$ for upper gerade states (solid lines). (b) Measured absorption coefficient of Cs vapor at ($T = 290\ ^\circ\text{C}$) in the vicinity of the D1 ($6\ ^2S_{1/2} + 6\ ^2P_{1/2}$) and D2 ($6\ ^2S_{1/2} + 6\ ^2P_{3/2}$) line.

because of the constant temperature and density of cesium atoms along the optical path.

2.2 Absorption spectra

The absorption measurements were performed in the temperature range from $200\ ^\circ\text{C}$ ($N_{\text{Cs}} = 1.62 \times 10^{15}\ \text{cm}^{-3}$ [18]) to $300\ ^\circ\text{C}$ ($N_{\text{Cs}} = 3.19 \times 10^{16}\ \text{cm}^{-3}$). Above $300\ ^\circ\text{C}$ the absorption due to the wings of the D1 and the D2 lines becomes very large, the molecular absorption due to the $\text{Cs}_2 A-X$ band becomes significant, and the observation of the 875.2 nm satellite band is obstructed.

The cesium absorption coefficient was determined in the wavelength region from 815 nm to 930 nm. Figure 3b shows the cesium absorption coefficient at the temperature of $290\ ^\circ\text{C}$ ($N_{\text{Cs}} = 2.49 \times 10^{16}\ \text{cm}^{-3}$). The group of four satellite bands in the far blue wing of D2 line [9], the inner-wing satellites of the D1 and D2 lines (891.4 nm [2, 3] and 857.3 nm [19]) the molecular $X\ ^1\Sigma_g^+ \rightarrow A\ ^1\Sigma_u^+$ band and the satellite at 875.2 nm are clearly resolved. In Figure 3a the cesium difference potential curves that fit into the measured wavelength interval are shown. These difference potentials are calculated from the *ab initio* potential curves [1]. The correspondence between various extrema of the difference potential curves in Figure 3a, and the observed satellite bands shown in Figure 3b is evident. In particular, the 875.2 nm satellite corresponds to the maximum in the 0_g^+ ($6\ ^2S_{1/2} + 6\ ^2P_{1/2}$) - 1_u ($6\ ^2S_{1/2} + 6\ ^2S_{1/2}$) difference potential located at the internuclear distance of 19 Bohr, indicated by the horizontal arrow in Figure 3.

3 Theory

We used the semiclassical approach for the calculation of the absorption coefficient. Absorption spectra of the optical transitions from the initial molecular state with electronic energy $V_i(R)$ to the final molecular state with the electronic energy $V_f(R)$ in the case of the weak field were described in the simplest quasistatic approximation. The linear absorption coefficient $k(\omega)$ was obtained by the following well-known relation (see *e.g.* [20]):

$$k(\omega) = N^2 \frac{4\pi^2 e^2 \hbar}{mc} \sum_c \frac{R_c^2 f(R_c)}{|\Delta'(R_c)|} \exp(-V_i(R_c)/kT). \quad (1)$$

N is the atom number density, T is the temperature of the vapor and $\Delta(R)$ is the difference potential $\Delta(R) = V_f(R) - V_i(R)$. The summation in the relation (1) is taken over all Condon points R_c which satisfy the condition:

$$\Delta(R_c) = \hbar\omega. \quad (2)$$

$\Delta'(R_c) = (d\Delta(R)/dR)_{R=R_c}$ is the first derivative of the difference potential. The molecular oscillator strength $f(R_c)$ [20] at the Condon point R_c is defined by the relation:

$$f(R_c) = \frac{2m\omega}{3\hbar e^2 g_i} \sum_{\alpha,\beta} |\mathbf{D}_{\alpha\beta}(R_c)|^2, \quad (3)$$

where g_i is the statistical weight of the initial state and $\mathbf{D}_{\alpha\beta}(R_c)$ is the matrix element of the electric dipole moment for the electronic transition between initial substate α to the final substate β .

The absorption coefficient calculated in quasistatic approximation by using the relation (1) shows a singularity at the extremum in the difference potential. In this case it is essential to use the Airy approximation of the linear absorption coefficient (see *e.g.* [19]) given by the following relation:

$$k(\omega) = N^2 \frac{12\pi^3 e^2 \hbar}{mc} \sqrt{\pi z} \left[\left(\frac{R_1^2 f(R_1)}{|\Delta'(R_1)|} \exp(-V_i(R_1)/kT) + \frac{R_2^2 f(R_2)}{|\Delta'(R_2)|} \exp(-V_i(R_2)/kT) \right) \left(L(z) + \frac{H(z)}{z} \right) + 2 \frac{R_1^2 F(R_1, R_2)}{\sqrt{|\Delta'(R_1)\Delta'(R_2)|}} \exp(-V_i(R_1)/kT) \times \left(L(z) - \frac{H(z)}{z} \right) \right]. \quad (4)$$

The relation (4) can be applied to the difference potentials where for each frequency ω exist two real solutions of the equation (2). The first term in the square bracket of equation (4) describes the contribution of each Condon point, while the second term describes their interference. The function $F(R_1, R_2)$ in the interference term of relation (4) is analog to the molecular oscillator strength function $f(R)$

$$F(R_1, R_2) = \frac{2m\omega}{3\hbar e^2 g_i} \sum_{\alpha,\beta} \mathbf{D}_{\alpha\beta}(R_1) \cdot \mathbf{D}_{\alpha\beta}(R_2). \quad (5)$$

The functions $L(z)$ and $H(z)$ [19,21,22] are given by the following relations:

$$L(z) = \int_0^\infty dt e^{-1/t^3} \frac{[\text{Ai}(-zt)]^2}{t^2},$$

$$H(z) = \int_0^\infty dt e^{-1/t^3} \frac{[\text{Ai}'(-zt)]^2}{t^3}, \quad (6)$$

where $\text{Ai}(-zt)$ and $\text{Ai}'(-zt)$ are the Airy function and its first derivative.

The argument z is the function of the phase difference between two Condon points at a given frequency ω :

$$z(\omega) = \left(\frac{\mu}{2kT} \right)^{\frac{1}{3}} \left(\frac{3}{4\hbar} \int_{R_1}^{R_2} dR (\Delta(R) - \hbar\omega) \right)^{\frac{2}{3}}, \quad (7)$$

where μ is the reduced molecular mass.

The total linear absorption coefficient is calculated as a sum of absorption coefficients of all different transitions that contribute independently to the spectral region of interest:

$$k(\omega) = \sum_{i,f} k_{if}(\omega) \quad (8)$$

The comparison of the calculated linear absorption coefficient with the experiment in a wavelength region between cesium D1 and D2 lines for the temperature of 290 °C is shown in Figure 4 (note logarithmic scale for k (cm^{-1})). The calculations were performed for the $1_u, 0_u^-$ ($6^2S_{1/2} + 6^2S_{1/2}$) \rightarrow 1_g ($6^2S_{1/2} + 6^2P_{3/2}$) and 0_g^+ ($6^2S_{1/2} + 6^2S_{1/2}$) \rightarrow 0_u^+ ($6^2S_{1/2} + 6^2P_{3/2}$) transitions using the relation (1). In view of the extensive averaging inherent in thermal collisions, calculations using the semiclassical approach are fully adequate. The contributions caused by the $1_u, 0_u^-$ ($6^2S_{1/2} + 6^2S_{1/2}$) \rightarrow 0_g^- ($6^2S_{1/2} + 6^2P_{3/2}$), 1_u ($6^2S_{1/2} + 6^2S_{1/2}$) \rightarrow 0_g^+ ($6^2S_{1/2} + 6^2P_{1/2,3/2}$) and 0_g^+ ($6^2S_{1/2} + 6^2S_{1/2}$) \rightarrow 1_u ($6^2S_{1/2} + 6^2P_{1/2}$) transitions were calculated by using the relation (4). It is evident that the experimental coefficient of absorption is well reproduced by the theoretical profile. The 857.3 nm [19] and 891.4 nm [2,3] measured satellite bands which are connected with the minimum in the difference potential of the $1_u, 0_u^-$ ($6^2S_{1/2} + 6^2S_{1/2}$) \rightarrow 0_g^- ($6^2S_{1/2} + 6^2P_{3/2}$) transition and the maximum in the difference potential of the 0_g^+ ($6^2S_{1/2} + 6^2S_{1/2}$) \rightarrow 1_u ($6^2S_{1/2} + 6^2P_{1/2}$) transition, respectively, are in excellent agreement with our simulation.

The shape of the 875.2 nm satellite band is well reproduced by the calculations, although the position of the theoretical band peak is a bit shifted to the larger wavelength. This is caused by small shift of about -15 cm^{-1} of the difference potential maximum. The maximum in the difference potential of the 1_u ($6^2S_{1/2} + 6^2S_{1/2}$) \rightarrow 0_g^+ ($6^2S_{1/2} + 6^2P_{1/2}$) transition which is responsible for the appearance of this satellite band is a consequence of the avoided crossing of two 0_g^+ adiabatic potential curves. In the region of this avoided crossing the value of the

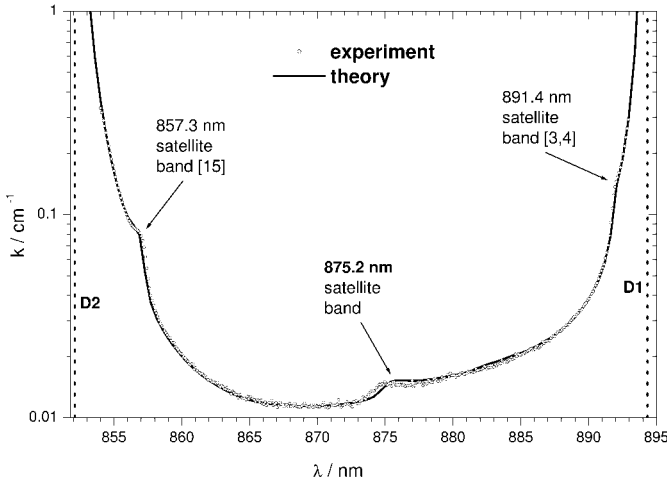


Fig. 4. Comparison of measured and calculated absorption coefficients in the spectral region between Cs D1 and D2 line. The Cs_2 857.3 nm, 875.2 nm and 891.4 nm satellite bands are visible in the spectrum.

Π/Σ spin-orbit interaction is different from its asymptotic value. A small inaccuracy in the *ab initio* calculation of the spin-orbit interaction in the region of the avoided crossing might be one of the possible reasons of the modest difference in the theoretical and experimental positions of satellites peak. More likely, we may conclude that our potential implies a smaller C_3 constant of the repulsive resonance interaction curve. Indeed, our C_3 constant for the $^3\Pi_g$ state equals 9.90 a.u., whereas reliable calculations of Marinescu and Dalgarno reveal 10.47 a.u. [23]. Fioretti *et al.* used two different fit procedures in the analysis of the ro-vibrational levels of 0_g^- state not sufficiently close to the dissociation energy and deduced two values for the C_3 constant, 9.84 a.u. and 11.61 a.u. [24]. Actually, using the value 10.47 a.u. would exactly bring about the desired shift of 15 cm^{-1} . Thus our measurements appear to support the C_3 constant value from Marinescu and Dalgarno [23].

4 Discussion

The comparison of the measured and calculated absorption coefficient in the close neighborhood of the 875.2 nm satellite band is shown in Figure 5. There are only three transitions relevant for the formation of the spectra in this wavelength region. Their contributions to the total absorption coefficient are separately shown in this figure. At the given temperature, the main contribution to the spectrum arises from the 0_g^+ ($6^2S_{1/2}$ + $6^2S_{1/2}$) \rightarrow 0_u^+ ($6^2S_{1/2}$ + $6^2P_{3/2}$) transition. This transition together with the $1_u, 0_u^-$ ($6^2S_{1/2}$ + $6^2S_{1/2}$) \rightarrow 1_g ($6^2S_{1/2}$ + $6^2P_{3/2}$) form a background on which the contribution from the 1_u ($6^2S_{1/2}$ + $6^2S_{1/2}$) \rightarrow 0_g^+ ($6^2S_{1/2}$ + $6^2P_{1/2}$) transition, responsible for the formation of the 875.2 nm satellite band, is superimposed.

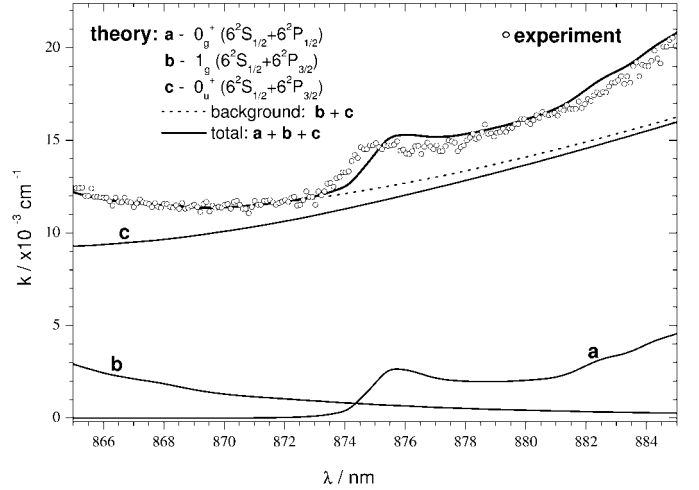


Fig. 5. The enlarged part of Figure 4 showing experimental and simulated absorption coefficients in the region of the 875.2 nm satellite band. Only three potentials contribute to the absorption coefficient in this region. The shape of the satellite is dominated by the absorption to the 0_g^+ ($6^2S_{1/2}$ + $6^2P_{1/2}$) upper state (curve a). The combined absorption to the 0_u^+ ($6^2S_{1/2}$ + $6^2P_{3/2}$) state (curve c) and to the 0_g^+ ($6^2S_{1/2}$ + $6^2P_{3/2}$) states (curve b) represents the background (dotted line).

We would like to point out the possible use of the 0_g^+ ($6^2S_{1/2}$ + $6^2P_{1/2}$) state in the formation of ultracold Cs_2 molecules using two-step excitation. In the first excitation step, at intermediate long-range distances, there is still allowed transition 1_u ($6^2S_{1/2}$ + $6^2S_{1/2}$) \rightarrow 0_g^+ ($6^2S_{1/2}$ + $6^2P_{1/2}$) to a narrow range of quasibound states at the inner side of the barrier. Then, in a second step, from the inner turning point of the Cs_2 $2^1\Sigma_g^+$ almost metastable state, another photon of different energy, excites a higher $^1\Sigma_u^+$ or $^1\Pi_u$ state from which the radiative transition down towards Cs_2 $1(X)^1\Sigma_g^+$ ultracold state would be possible [25,26]. Arrows 1, 2 and 3 in Figure 6 schematically show the processes. It should be noted that the highest $^1\Sigma_u^+$ or $^1\Pi_u$ states mentioned in this scheme exist and some of them have been already calculated [1]. They should have relatively long lifetime and negligible predissociation.

Much in the same way there is another allowed transition 1_u ($6^2S_{1/2}$ + $6^2S_{1/2}$) \rightarrow 0_g^+ ($6^2S_{1/2}$ + $6^2P_{3/2}$), also on the left side of the barrier in this state. Again, a photon of different energy may be used to excite even higher excited $^1\Sigma_u^+$ or $^1\Pi_u$ states, from which a Cs_2 $1(X)^1\Sigma_g^+$ ultracold state could be formed by spontaneous emission. However, the spontaneous transition from the inner turning point of the 0_g^+ ($1^3\Pi_g, 6^2S_{1/2}$ + $6^2P_{3/2}$) state may be used for the formation of the ultracold Cs_2 $1(a)^3\Sigma_u^+$ molecules, shown by arrows 1' and 2' in Figure 6. All these processes may be checked in relatively dense ultracold cesium MOT devices.

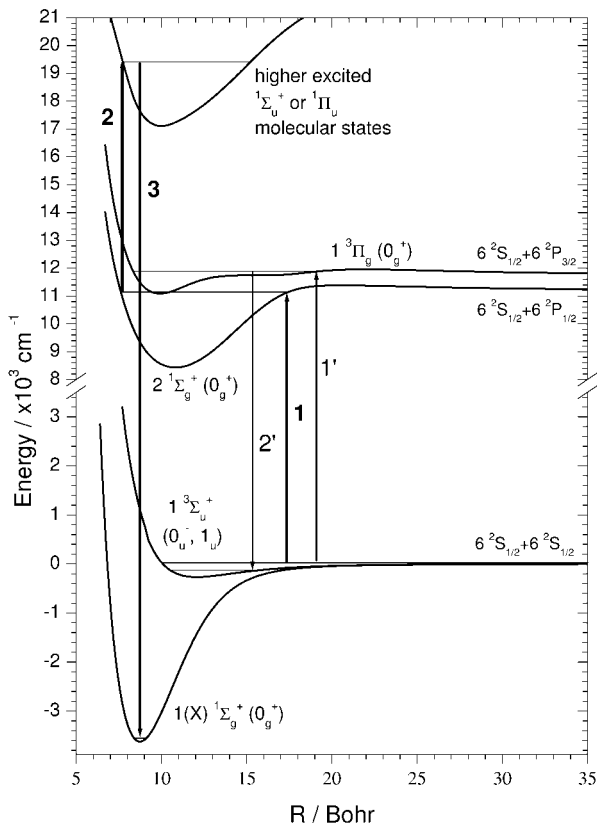


Fig. 6. Partial energy diagram for the Cs_2 molecule showing proposed excitation and emission processes involved in the formation of the ultracold Cs_2 $1(X) \ ^1\Sigma_g^+$ or Cs_2 $1(a) \ ^3\Sigma_u^+$ molecules via 0_g^+ ($6 \ ^2S_{1/2} + 6 \ ^2P_{1/2}$) and 0_g^+ ($6 \ ^2S_{1/2} + 6 \ ^2P_{3/2}$) intermediate states.

5 Conclusion

We performed emission and absorption measurements of Cs satellite band at 875.2 nm. Theoretical calculations of the satellite profile at 875.2 nm show satisfactory agreement with the measured absorption profiles.

We propose the use of collisions between the two ultra cold ground state cesium atoms for the formation of ultracold Cs_2 molecules in $1(X) \ ^1\Sigma_g^+$ or $1(a) \ ^3\Sigma_u^+$ molecular states using the intermediate long-range region of Cs_2 0_g^+ ($6 \ ^2S_{1/2} + 6 \ ^2P_{1/2}$) and 0_g^+ ($6 \ ^2S_{1/2} + 6 \ ^2P_{3/2}$) states.

We greatly acknowledge the kind help of Prof. K. Günther (OSRAM, Berlin) for giving us an experimental pulsed cesium high-pressure lamp with all physical information. This work was supported by Ministry of Science and Technology of Republic of Croatia (Program/Theme 00350101/2).

References

1. N. Spies, Ph.D. thesis, Fachbereich Chemie, Universität Kaiserslautern, 1989; W. Meyer, N. Spies, to be published.
2. A.N. Klucharev, A.V. Lazarenko, G. Pichler, M. Movre, Phys. Lett. A **61**, 104 (1977).
3. K. Niemax, G. Pichler, J. Phys. B: At. Mol. Phys. **7**, 2355 (1974).
4. D. Veža, M. Movre, G. Pichler, J. Phys. B: At. Mol. Phys. **13**, 3605 (1980).
5. M. Movre, G. Pichler, J. Phys. B: At. Mol. Phys. **10**, 2631 (1977).
6. W.C. Stwalley, H. Wang, J. Mol. Spectrosc. **195**, 194 (1999).
7. O. Dulieu, R. Kosloff, F. Masnou-Seeuws, G. Pichler, J. Chem. Phys. **107**, 10633 (1997).
8. G. Pichler, M. Movre, D. Veža, K. Niemax, in *Proc. 33rd Symp. On Molec. Spectroscopy* (Columbus, Ohio, June 12-16, 1978), TF 11.
9. D. Veža, R. Beuc, S. Milošević, G. Pichler, Eur. Phys. J. D **2**, 45 (1998).
10. G. Herzberg, *Molecular spectra and molecular structure, I Diatomic molecules* (Van Nostrand, New York, 1945).
11. J. van Neumann, E. Wigner, Z. Phys. **30**, 467 (1929).
12. J.S. Cohen, B. Schneider, J. Chem. Phys. **61**, 3240 (1974).
13. D.H. Sarkisyan, A.S. Sarkisyan, A.K. Yalanusyan, Appl. Phys. B **66**, 241 (1998).
14. T. Ban, H. Skenderović, R. Beuc, G. Pichler, Europhys. Lett. **48**, 378 (1999).
15. T. Ban, S. Ter-Avetisyan, R. Beuc, H. Skenderović, G. Pichler, Chem. Phys. Lett. **313**, 110 (1999).
16. T. Ban, H. Skenderović, S. Ter-Avetisyan, G. Pichler, published online in Appl. Phys. B, DOI: 10.1007/s003400000488.
17. J. Liu, Ph.D. thesis, Berlin, 1998.
18. A.N. Nesmeyanov, in *Vapor Pressure of Elements* (Academic Press, New York, 1963).
19. R. Beuc, V. Horvatić, J. Phys. B: At. Mol. Opt. Phys. **25**, 1497 (1992).
20. M. Movre, G. Pichler, J. Phys. B: At. Mol. Phys. **10**, 2631 (1977).
21. J. Szudy, W.E. Baylis, J. Quant. Spectrosc. Transfer **15**, 641 (1975).
22. P.A. Vicharely, C.B. Collins, in *Spectral Line Shape*, edited by K. Burnett (de Gruyter, Berlin, 1985), Vol. 2, p. 537.
23. M. Marinescu, A. Dalgarno, Phys. Rev. A **52**, 311 (1995).
24. A. Fioretti, D. Comparat, C. Drag, C. Amiot, O. Dulieu, F. Masnou-Seeuws, P. Pillet, Eur. Phys. J. D **5**, 389 (1999).
25. A.N. Nikolov, J.R. Ensher, E.E. Eyler, H. Wang, W.C. Stwalley, P.L. Gould, Phys. Rev. Lett. **84**, 246 (2000).
26. M.-L. Almazor, O. Dulieu, F. Masnou-Seeuws, R. Beuc, G. Pichler, Eur. Phys. J. D **15**, (to be published, No. 3, 2001).